Rituximab (Chimeric Anti-CD20 Monoclonal Antibody) Inhibits the Constitutive Nuclear Factor-κB Signaling Pathway in Non-Hodgkin's Lymphoma B-Cell Lines: Role in Sensitization to Chemotherapeutic Drug-induced Apoptosis

Ali R. Jazirehi,[1] Sara Huerta-Yepez,[1,3] Genhong Cheng,[1,2] and Benjamin Bonavida[1]

[1]Department of Microbiology, Immunology, and Molecular Genetics and [2]Molecular Biology Institute, Jonsson Comprehensive Cancer Center, David Geffen School of Medicine at UCLA, University of California, Los Angeles, California and [3]Unidad de Investigacion Medica en Inmunologia e Infectologia, Hospital de Infectologia, "La Raza," CMN, Mexico City, Mexico

Abstract

The chimeric anti-CD20 antibody rituximab (Rituxan, IDEC-C2B8) is widely used in the clinical treatment of patients with non-Hodgkin's lymphoma (NHL). Rituximab sensitizes NHL B-cell lines to drug-induced apoptosis via down-regulation of Bcl-x_L expression. We hypothesized that the mechanism by which rituximab down-regulates Bcl-x_L may be, in part, due to inhibition of constitutive nuclear factor-κB (NF-κB) activity that regulates Bcl-x_L expression. This hypothesis was tested in CD20$^+$ drug-resistant Ramos (Bcl-2$^-$/Bcl-x_L^+) and Daudi (Bcl-2$^+$/Bcl-x_L^+) cell lines. Rituximab decreased the phosphorylation of NF-κB-inducing kinase, IκB kinase, and IκB-α, diminished IKK kinase activity, and decreased NF-κB DNA binding activity. These events occurred with similar kinetics and were observed 3 to 6 hours post-rituximab treatment. Rituximab significantly up-regulated Raf-1 kinase inhibitor protein expression, thus interrupting the NF-κB signaling pathway concomitant with Bcl-x_L and Bfl-1/A1 down-regulation. The role of NF-κB in the regulation of Bcl-x_L transcription was shown using promoter reporter assays in which deletion of the two-tandem NF-κB binding sites in the upstream promoter region significantly reduced the luciferase activity. This was further corroborated by using IκB super-repressor cells and by NF-κB–specific inhibitors. The direct role of Bcl-x_L in drug resistance was assessed by using Bcl-x_L–overexpressing cells, which exhibited higher drug resistance that was partially reversed by rituximab. Rituximab-mediated inhibition of the NF-κB signaling pathway and chemosensitization was corroborated by the use of specific inhibitors. These findings reveal a novel pathway mediated by rituximab through Raf-1 kinase inhibitor protein induction that negatively regulates the constitutive NF-κB pathway and chemosensitization of the NHL B-cells. (Cancer Res 2005; 65(1): 264–76)

Introduction

Traditionally, non-Hodgkin's lymphoma (NHL) patients have been treated with standard chemotherapeutic regimens, which have offered partial responses and led to eventual relapse. Subsequent administration of higher doses of chemotherapy has proven to be more toxic and induce a response in only 30% to 40% of patients (1–3). This pattern of inevitable failure of standard therapies is due to the emergence of drug-resistant variants, which highlights the importance of the design of new treatment regimens. Monoclonal antibodies (mAb) targeted against specific surface markers that are less systematically toxic and less myelosuppressive have provided an alternative therapeutic approach to malignant diseases (1–3).

The developmentally regulated B-cell lineage restricted marker CD20 is expressed on the surface of ≥95% of NHLs. CD20 is neither shed from the cell surface (4) nor modulated or internalized on antibody binding (5) nor circulates as a free protein in the plasma that can bind to and block the efficacy of the anti-CD20 antibodies, making it an ideal target for immunotherapy. Rituximab, chimeric mouse anti-human CD20 mAb, Rituxan, IDEC-C2B8 (6), alone or combined with chemotherapy, is successfully used in the treatment of patients with follicular low-grade and aggressive diffuse large B-cell lymphoma (7, 8). *In vitro* treatment of CD20$^+$ NHL B-cells with monomeric rituximab kills tumor cells via induction of antibody-dependent cellular cytotoxicity and complement-dependent cytotoxicity (9).

We have reported that rituximab interferes with the intracellular signal transduction pathways and sensitizes NHL B-cell lines to chemotherapeutic drugs via selective down-regulation of Bcl-2 and Bcl-x_L (10, 11). Bcl-2 and Bcl-x_L exert their antiapoptotic effects mainly in the membrane of mitochondria by preventing loss of membrane potential, cytochrome *c* efflux on apoptotic stimuli, and initiation of apoptosis (12). Bcl-x_L is predominantly expressed in lymphomas (13) and protects the cells from drug cytotoxicity, thus conferring a multidrug resistance phenotype (12, 14–16).

The mechanism by which rituximab inhibits Bcl-x_L expression is unknown. Visual inspection and computer analysis have revealed nuclear factor-κB (NF-κB) binding sites on the Bcl-x promoter, and NF-κB is partly responsible for *Bcl-x_L* gene expression (17–23). In addition, activation of the NF-B pathway by various stimuli rescues tumor cells from drug-induced apoptosis via up-regulation of Bcl-x_L (21, 22). Thus, Bcl-x_L is a downstream target of the NF-B pathway (17–24). Hence, we hypothesized that rituximab-mediated Bcl-x_L down-regulation may be due to inhibition of the constitutive activity of the NF-B pathway by rituximab.

A negative regulatory role for the Raf-1 kinase inhibitor protein (RKIP) on the NF-κB pathway has been described (25). RKIP exerts its suppressive effect via physical association with NF-κB–inducing kinase (NIK), tumor growth factor-β activating kinase 1 (TAK1), and IκB kinase (IKK), thus rendering them incapable of relaying the signal to downstream molecules. Overexpression of RKIP decreases

Requests for reprints: Benjamin Bonavida, Department of Microbiology, Immunology, and Molecular Genetics, University of California at Los Angeles, 10833 Le Conte Avenue, A2-060 CHS, Los Angeles, CA 90095-1747. Phone: 310-825-2233; Fax: 310-206-2791; E-mail: bbonavida@mednet.ucla.edu.

NF-κB–dependent transcription (25). Thus, we further hypothesized that rituximab may up-regulate RKIP expression resulting in inhibition of the NF-κB pathway, diminished NF-κB–dependent Bcl-x_L expression, and chemosensitization of NHL B-cells.

This study tested the above hypotheses using the CD20$^+$ Ramos (Bcl-2$^-$/Bcl-x_L^+) and Daudi (Bcl-2$^+$/Bcl-x_L^+) NHL B-cells. The following questions were investigated: (*a*) Does rituximab inhibit NF-B activity? (*b*) Does rituximab inhibit the NF-κB signal transduction pathway? (*c*) Does rituximab up-regulate RKIP expression and enhance its association with signaling molecules, thus interfering with the activation of the NF-κB signaling pathway? (*d*) Do pharmacologic inhibitors of the NF-κB pathway mimic rituximab-mediated effects? (*e*) Does rituximab-mediated inhibition of NF-κB and Bcl-x_L expression regulate tumor cell resistance to chemotherapy?

Materials and Methods

Cell Lines and Plasmid Construction. The CD20$^+$ human Burkitt's lymphoma B-cell lines Daudi and Ramos (American Type Culture Collection, Bethesda, MD; refs. 26, 27) were maintained in RPMI 1640 (Mediatech, Washington, DC) supplemented with 10% (v/v) heat-inactivated fetal bovine serum (to ensure the absence of complement) as reported (11). For the generation of the Ramos and Daudi IκB mutant cells, the 5′-FLAG-tagged IκB mutant was fused in-frame to the 5′ end of the mutant estrogen receptor (ER) ligand binding domain, and the chimera was cloned into the *Hin*dIII/*Eco*RI sites of pcDNA3 to generate the pcDNA3-IκB-ER construct. For the generation of Bcl-x_L-overexpressing Ramos cells, the pEBB-puro-Bcl-x-HA construct was generated by PCR cloning of human Bcl-x, which was then inserted into the *Bam*HI and *Not*I sites of pEBB-puro-HA in-frame with the 3′ influenza hemagglutinin tag. The cells were then pulsed using electroporation at 250 V, 975 F and then selected and maintained in 2.5 μg/mL puromycin (Sigma, St. Louis, MO) or 1 mg/mL active G418 (Mediatech; ref. 21). Cultures were incubated in a controlled atmosphere incubator at 37°C with saturated humidity and an atmosphere of 95% air and 5% CO_2 at 0.5×10^6 cells/mL.

Reagents. Paclitaxel (6 mg/mL in DMSO, Bristol Myers Squibb, New York, NY) was diluted by medium. The DMSO concentration did not exceed 0.1% in any experiment. Rituximab (10 mg/mL) was obtained commercially. Mouse anti-Bcl-x_L, anti-Bfl-1/A1, and anti-NIK mAbs and rabbit anti-p-NIK (Thr^{559}) and anti-IκB-α polyclonal antibodies were purchased from Santa Cruz Biotechnology (Santa Cruz, CA). Mouse anti-p-IκB-α (Ser$^{32/36}$) and anti-actin mAbs were purchased from Imgenex (San Diego, CA) and Chemicon (Temecula, CA), respectively. Rabbit anti-RKIP polyclonal antibody was purchased from Zymed (San Francisco, CA). Rabbit anti-IKKβ and p-IKKα/β (Ser$^{180/181}$) polyclonal antibodies were obtained from Cell Signaling (Beverly, MA). Bay 11-7058 (28, 29), rabbit anti-high mobility group 1 and anti-TAK1 antibodies, and 4-hydroxytamoxifen (4-OHT) were purchased from Calbiochem (San Diego, CA). SN50 (AAVALLPAVLLALLAPVQRKRQKLMP; ref. 30) and 2-methoxyantimycin-A3 (2MAM-A3; ref. 31) were purchased from Biomol (Plymouth, PA). Dehydroxymethylepoxyquinomicin (DHMEQ; refs. 32, 33) was provided by Dr. Kazuo Manawa (Tokyo, Japan). *Cis*-platinum and etoposide were purchased from Sigma.

Luciferase Bcl-x Promoter Reporter Assay. A 650-bp region of the Bcl-x promoter spanning −640 to +9 relative to the transcriptional start site was inserted between *Xho*I and *Hin*dIII sites of the pGL2-Basic luciferase reporter vector to generate the Bcl-x wild-type (WT) promoter. The NF-κB mutant promoter (Bcl-x κB) contains an internal deletion spanning the two potential NF-κB *cis* elements from −84 to −46 relative to the transcriptional start site (21). Ramos and Daudi cells were transfected by electroporation at 270 V, 975 μF with 10 μg Bcl-x WT promoter, Bcl-x κB promoter, or empty plasmid. After transfection, the cells were cultured in 12-well plates and were allowed to recover for 36 hours. Then, the cells were either left untreated or treated with Bay 11-7085 (4 μmol/L) or rituximab (20 μg/mL) for 18 hours. Cells were then harvested in 1× lysis buffer, and luciferase activity was measured using an analytic luminescence counter Monolith 2010.

Immunoblotting Analysis for Protein Expression. This was done as reported (11, 34, 35).

Immunoprecipitation of RKIP. Cells (10^7) per treatment (with or without rituximab) were harvested and pelleted at 14,000 × *g* for 2 minutes. The resulting cell pellets were resuspended and dissolved in 500 μL ice-cold radioimmunoprecipitation assay buffer. The supernatants were incubated overnight at 4°C on a shaking platform with 2 μg anti-NIK, anti-TAK1, and anti-IKK antibodies and were subsequently incubated with 30 μL ImmunoPure Plus Immobilized protein A (Pierce, Rockford, IL; ref. 36) for 4 hours at 4°C on a shaking platform. The supernatants were centrifuged for 1 minute at 14,000 × *g*, and the immunoprecipitates were washed twice with 1.0 mL of ice-cold radioimmunoprecipitation assay buffer prior to assay. RKIP was immunoprecipitated from the lysate by a rabbit anti-RKIP antibody. The immunoprecipitates were resolved on 10% SDS-PAGE and visualized by autoradiography.

Assessment of Apoptosis

DNA Fragmentation Assay. The percentage of apoptotic cells was determined by evaluation of propidium iodide (PI)–stained preparations (37) of tumor cells treated under various conditions as described (11, 34, 35). Cell cycle analysis and apoptosis were determined using an EpicXL flow cytometer. Cellular debris was excluded from analysis by raising the forward scatter threshold, and the DNA content of the intact nuclei was recorded on a logarithmic scale (37). Percentage apoptosis is represented as the percentage of hypodiploid cells accumulated at the sub-G_0 phase of the cell cycle.

Evaluation of Active Caspase-3 Levels. To validate the PI technique for the measurement of apoptosis, levels of active caspase-3 were evaluated with the FITC-labeled anti-active caspase-3 mAb. Pure IgG was used as isotype control (35).

2,3-Bis[2-Methoxy-4-Nitro-5-Sulfophenyl]-2*H*-Tetrazolium-5-Carboxanilide Inner Salt Proliferation Assay. Inhibition of proliferation was assessed using the standard XTT assay kit (Roche, Indianapolis, IN) that measures the metabolic activity of viable cells (38). The percentage of proliferation was calculated using the background-corrected reading as follows: % Proliferation = [(Absorbance of Sample Wells) / (Absorbance of Untreated Cells)] × 100.

Electrophoretic Mobility Shift Assay. Alterations in the DNA binding activity (DBA) of NF-κB were evaluated with biotin-labeled oligonucleotide NF-κB probe (5′-AGTTGAGGGGACTTTCCCAGGC-3′; ref. 39) using the electrophoretic mobility shift assay kit (Panomics, Inc., Redwood City, CA) as reported (35). For supershifts, 1 μL of the appropriate antibodies was added to the nuclear extracts for 20 minutes on ice before the addition of the labeled probe. The nuclear levels of high mobility group 1 were assessed to ensure equal loading.

Reverse Transcription-PCR. Transcriptional regulation of Bcl-x_L was detected by reverse transcription-PCR (11) using gene-specific primers: forward 5′-ACCATGTCTCAGAGCAACCGGGAGCT-3′ and reverse 5′-TCATTTCCGACTGAAGAGTGAGCC-3′. Internal control for equal cDNA loading was assessed using the gene-specific glyceraldehyde 3-phosphate dehydrogenase primers: forward 5′-GAACATCATCCCTGCCTCTACTG-3′ and reverse 5′-GTTGCTGTAGCCAAATTCGTTG-3′. Amplifications were carried out using HotStart/Ampliwax method (40) with the temperature cycling variables: 95°C, 1 minute; 60°C, 1 minute; 35 cycles. Amplicons were analyzed on 2% agarose gels and the relative concentrations of the bands were assessed by densitometric analysis of the digitized ethidium bromide–stained images using the NIH image program. The intensity of each band was normalized to that of the corresponding glyceraldehyde 3-phosphate dehydrogenase.

Immune Complex Kinase Assay. Alteration in the kinase activity of IKK by rituximab was assessed by its ability to phosphorylate IκB-α (Ser$^{32/36}$) using a slightly modified version of previous methods (41). Briefly, cells were grown with or without 20 μg/mL rituximab for 24 hours. Then, the cells were lysed in modified radioimmunoprecipitation assay buffer [50 mmol/L Tris-HCl (pH 7.5), 150 mmol/L NaCl, 1% Igepal CA-630, 0.25% sodium deoxycholate, 1 mmol/L EGTA, 5 mmol/L NaF, 1 mg/mL leupeptin and pepstatin, 1 mg/mL aprotinin, 1 mmol/L Na_3VO_4, 1 mmol/L phenylmethylsulfonyl fluoride]. The lysates were incubated with 2 μg anti-IKK antibody at 4°C on a shaking platform (overnight). IKK was immunoprecipitated from the lysates by subsequently incubating the lysates with 30 μL Immuno-Pure Plus Immobilized protein A (36) for 4 hours at 4°C on a shaking platform. The lysates were then centrifuged for 1 minute at 14,000 × *g*, the supernatant was discarded, and the immunoprecipitates were washed twice with 1.0 mL ice-cold modified radioimmunoprecipitation assay buffer followed by two to three washes with 1.0 mL ice-cold kinase binding buffer [20 mmol/L HEPES (pH 7.6), 50 mmol/L NaCl, 0.05% Igepal CA-630, 0.1 mmol/L EDTA, 2.5 mmol/L $MgCl_2$] prior to assay. Samples were then incubated with 35μL kinase reaction buffer [20 mmol/L HEPES (pH 7.6), 20 mmol/L $MgCl_2$, 20 mmol/L β-glycerophosphate, 20 mmol/L *p*-nitrophenyl phosphate, 0.5 mmol/L Na_3VO_4, 15 μmol/L ATP, 2 mmol/L DTT] containing a final concentration of 5 μg per sample IκB-α peptides (amino acids 1-50 and 1-50 $Ser^{32/36A}$) and 20 μmol/L ATP for 30 minutes at 30°C with gentle agitation of the settled beads every 10 minutes. Then, 2× SDS-PAGE sample buffer (35 μL) was added and the samples were boiled at 100°C for 3 to 5 minutes and the supernatants were electrophoresed on 10% SDS-PAGE and subjected to immunoblotting using anti-p-IκB-α ($Ser^{32/36}$) mAb.

Statistical Analysis. Assays were set up in triplicates and the results were expressed as means ± SD. Statistical analysis and *P* determinations were done by two-tailed paired *t* test with 95% confidence interval for determination of the significance of differences between the treatment groups. $P < 0.05$ was considered significant. ANOVA was used to test the significance among the groups. The InStat 2.01 software was used for analysis.

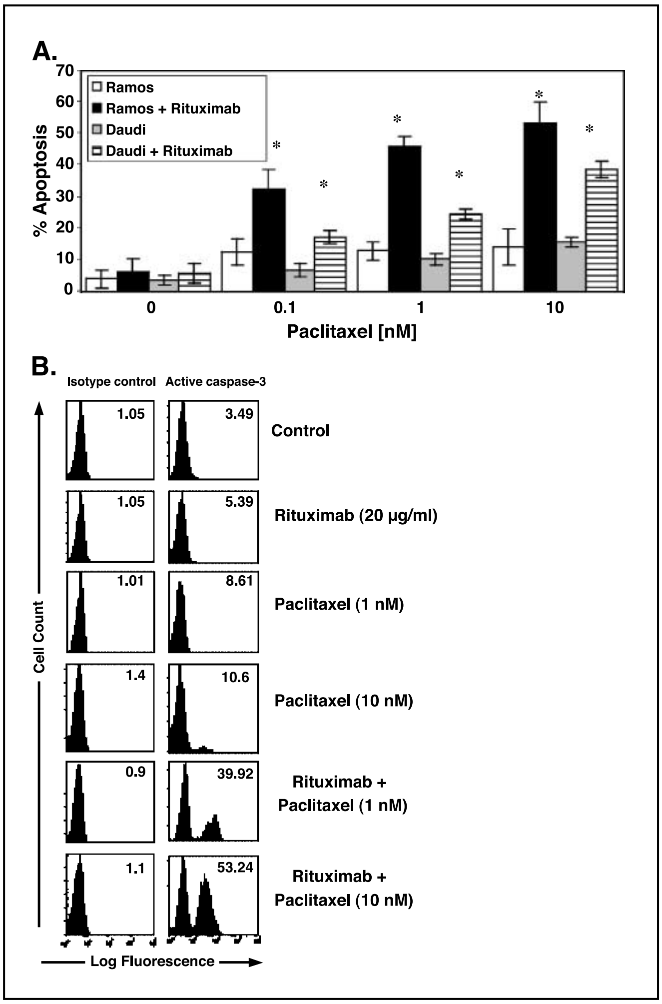

Figure 1. Rituximab sensitizes the NHL B-cells to drug-induced apoptosis. *A,* tumor cells (2 × 10^6) were left either untreated or treated with rituximab (20 μg/mL, 24 hours). Then, the cells were washed, fresh medium was added, and cells were incubated with various concentrations of paclitaxel (0.1-10 nmol/L, 18 hours). Then, the cells were stained with PI solution and cell cycle analysis and apoptosis were assessed by flow cytometry. Percentage of apoptosis is represented as the percentage of tumor cells with hypodiploid DNA accumulating at the sub-G_0 phase of the cell cycle. Samples were set up in triplicates. *Columns,* mean of two independent experiments; *bars,* SD. *B,* an aliquot of Ramos cells (*A*) was stained with FITC-labeled anti-active caspase-3 mAb to assess the levels of active caspase-3. Representative of two independent experiments. *, $P < 0.05$, compared with paclitaxel treatment alone.

Results

Rituximab Sensitizes Ramos and Daudi NHL B-Cells to Drug-Induced Apoptosis. Previous findings have shown that rituximab sensitizes NHL B-cell lines to apoptosis induced by various chemotherapeutic drugs (cisplatin, Adriamycin, vinblastine, 5-fluorouracil, and paclitaxel; refs. 10, 11). Paclitaxel was used as a representative drug in delineating rituximab-mediated signaling. To assess the chemosensitizing attribute of rituximab, Ramos and Daudi cells were left either untreated or pretreated with the optimal concentration of rituximab (20 μg/mL; ref. 42) for 24 hours. Cells were then washed and fresh medium was added, incubated with various concentrations of paclitaxel (0.1, 1, and 10 nmol/L, 18 hours), and subjected to PI staining (DNA fragmentation assay). The percentage apoptosis is represented as the percentage of hypodiploid cells accumulating at the sub-G_0 phase of the cell cycle. Rituximab alone did not induce significant apoptosis beyond the background levels in both cell lines. However, all three concentrations of paclitaxel induced significant apoptosis in rituximab-pretreated Ramos and Daudi cells compared with the untreated cells, albeit to varying degrees (Fig. 1*A*). The augmentation of apoptosis was synergistic as assessed by isobolographic analysis (ref. 11; data not shown). To further confirm the results of apoptosis achieved by DNA hypodiploidy, the levels of activated caspase-3 were measured. Substantial activation of caspase-3 was only observed in Ramos cells treated with combination of rituximab and paclitaxel and was not detected by each agent used alone (Fig. 1*B*). Activation of caspase-3 closely correlated with the percentage of the hypodiploid cells (PI^+) accumulated at the sub-G_0 region. Because paclitaxel at a 10 nmol/L concentration in combination with rituximab induced the highest level of apoptosis, this concentration was chosen for the subsequent experiments.

Rituximab Down-Regulates Bcl-x_L and Bfl-1/A1 Expression in Ramos and Daudi NHL B-Cells. Tumor cells were grown either in complete medium or in complete medium supplemented with rituximab (20 μg/mL, 24 hours). Total RNA was extracted and converted to first-strand cDNA. The cDNA (2.5 μg) of each condition was subjected to reverse transcription-PCR analysis using Bcl-x_L mRNA-specific primers. As shown, in Bcl-2–deficient Ramos cells (43) and Bcl-2–expressing Daudi cells, rituximab decreased the transcription of Bcl-x_L (Fig. 2*A*). Temporal regulation of rituximab-mediated inhibition of *Bcl-x_L* gene expression occurred in a time-dependent manner and was detected as early as 1 hour post-rituximab treatment, an effect that was more pronounced during later time points (Fig. 2*B*). Immunoblot analysis of total cell lysates of rituximab-treated (20 μg/mL, 24 hours) Ramos and Daudi cells revealed that rituximab decreased the protein levels of Bcl-x_L and Bfl-1/A1 in both cell lines (Fig. 2*C*) while having no effect on the expression of several other apoptosis-associated gene products tested (ref. 11; data not shown). These results show the ability of rituximab to down-regulate the expression of Bcl-x_L and Bfl-1/A1 in Ramos and Daudi NHL B-cells, both of which are regulated by NF-κB (20–23).

Rituximab Inhibits the Constitutive Activity of NF-κB and the NF-κB Signaling Pathway

Inhibition of the Signaling Pathway. We next examined the alteration in the DBA of NF-κB on rituximab treatment. After overnight growth in RPMI 1640 with 1% heat-inactivated fetal bovine serum, the cells were washed, fresh (complete) medium was added, and the cells were left either untreated or treated with rituximab (20 μg/mL, 1-24 hours). Nuclear extracts were prepared and biotin-labeled oligonucleotides comprising the NF-κB consensus binding site (39) were used as probe in an electrophoretic mobility shift assay. Time kinetics studies reveal that NF-κB DBA was diminished in the presence of rituximab as early as 3 to 6 hours post-treatment (Fig. 3), which remained decreased in the presence of rituximab during the entire experiment (24 hours). Rituximab-mediated decrease in NF-κB DBA was corroborated by the use of the NF-κB inhibitor Bay 11-7085 (4 μmol/L, 1 hours). The specificity of the electrophoretic mobility shift assay was corroborated using no nuclear extracts, positive control, unrelated probe, and unlabeled cold probe. The postulated NF-κB bands showed significant shift following the addition of the p65 and p50 antibodies to the nuclear extracts, confirming the involvement of NF-κB. The nuclear levels of the high mobility group 1 protein were confirmed for equal loading of the samples (Fig. 3).

Because rituximab-treated cells exhibited decreased NF-κB DBA, we analyzed the effect of rituximab on the NF-κB pathway. Cells were grown overnight in RPMI 1640 with 1% heat-inactivated fetal bovine serum. Then, the cells were washed and were grown either in complete medium or in complete medium supplemented with rituximab (20 μg/mL, 1-24 hours). Subsequently, total cell lysates (40 μg) were subjected to immunoblotting using phosphospecific and nonphosphospecific antibodies for proteins in the NF-κB pathway. As shown, rituximab treatment decreased the phosphorylation-dependent state of NIK, IKK, and IκB-α in a time-dependent manner beginning 3 to 6 hours post-treatment, which

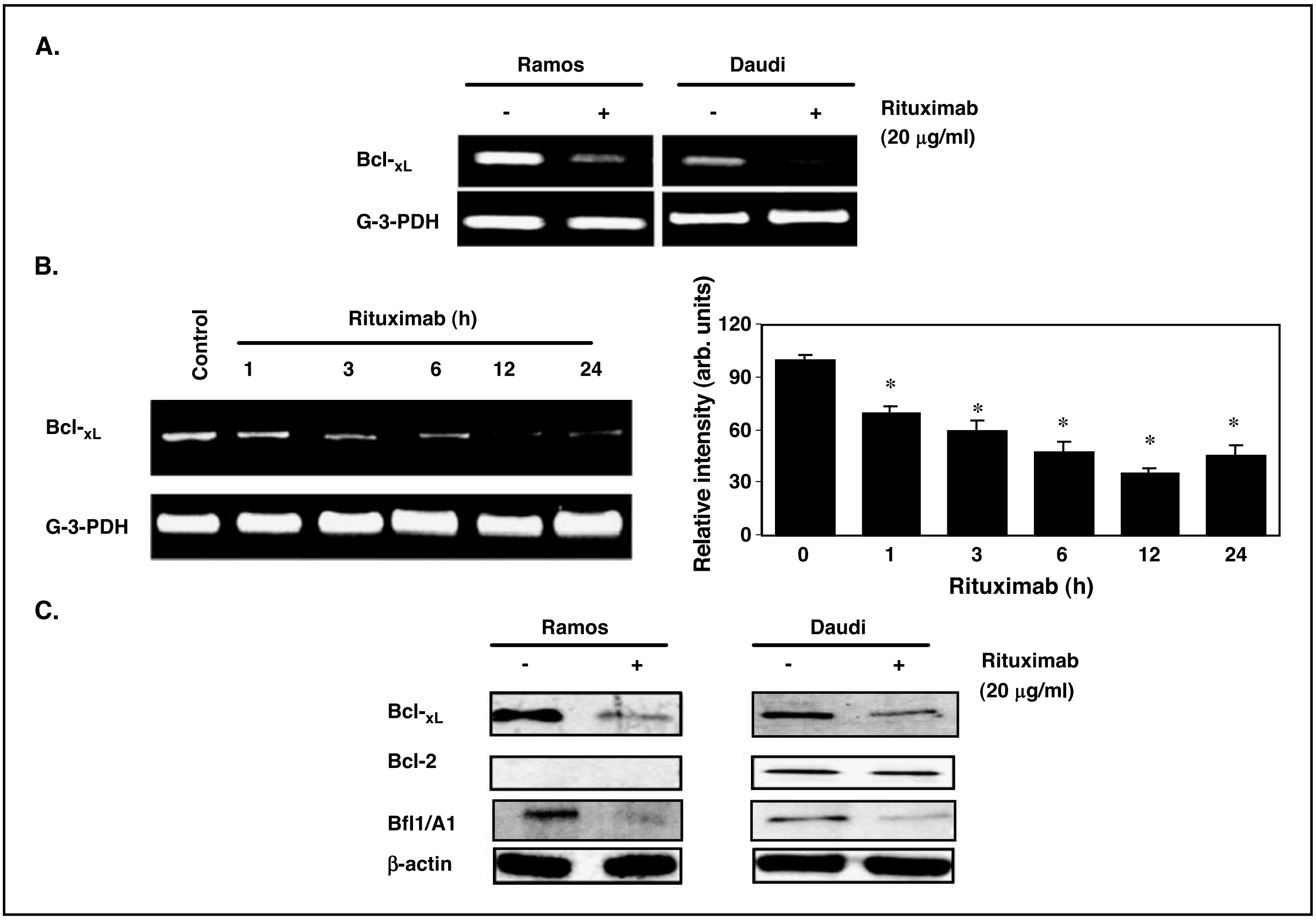

Figure 2. Rituximab inhibits Bcl-x_L and Bfl-1/A1 expression in the NHL B-cell lines. *A,* Ramos and Daudi cells were left either untreated (*Control*) or pretreated with rituximab (20 μg/mL, 24 hours). Total RNA was extracted and reverse transcribed to first-strand cDNA. cDNA (2.5 μg) of various sample conditions was used in PCR analysis. *B,* Ramos cells were treated with rituximab (20 μg/mL) for various time points and PCR was carried out as described in *A. C,* total cell lysates (40 μg) of Ramos and Daudi cells (±20 μg/mL rituximab, 24 hours) were subjected to immunoblotting and analyzed for Bcl-x_L, Bcl-2, and Bfl-1/A1 (*n* = 2). Intensity of the bands was normalized to that of the corresponding glyceraldehyde 3-phosphate dehydrogenase (*G-3-PDH*). *Columns,* mean of two independent experiments; *bars,* SD. *, $P < 0.05$, compared with control.

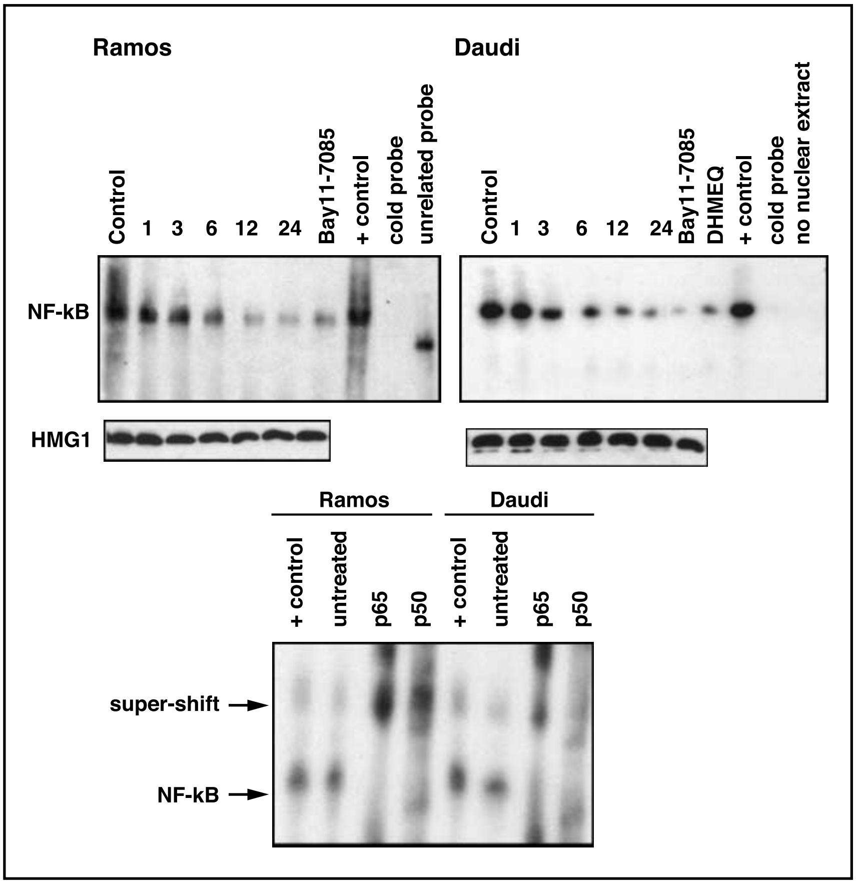

Figure 3. Rituximab diminishes NF-κB DBA in NHL B-cells. After overnight growth in RPMI 1640 + 1% fetal bovine serum, Ramos and Daudi cells were washed and grown in complete medium ± rituximab or Bay 11-7058. Nuclear lysates (10 μg) were subjected to electrophoretic mobility shift assay. Specificity of the assay was confirmed by the inclusion of appropriate controls. Levels of high mobility group 1 (*HMG1*) were confirmed for equal loading of the nuclear extracts. For supershifts, 1 μL of anti-p50 and anti-p65 antibodies was added to the nuclear extracts 20 minutes before the addition of labeled probe. Representative of two independent experiments.

was maintained up to 24 hours. The basal level (phosphorylation-independent state) of these signaling proteins remained unaltered during the entire (24 hours) experiment (Fig. 4*A*). The above findings denote the ability of rituximab to dephosphorylate the components of the NF-κB pathway. To ascertain whether the observed dephosphorylation also resulted in decreased kinase activity of the NF-κB pathway, an immune complex kinase assay was done. The IKK kinase activity of tumor cells (with or without rituximab 20 μg/mL, 24 hours) was assessed using IκB-α peptide (amino acids 1-50 $Ser^{32/36}$) as substrate. Rituximab decreased the IKK kinase activity as shown by the reduced ability of rituximab-treated lysates to phosphorylate IκB-α. This phenomenon was not observed when IB-α peptide (amino acids 1-50 $Ser^{32/36A}$) was used as substrate (Fig. 4*B*). These results denote the ability of rituximab to negatively regulate the activity of the NF-κB signaling pathway.

Biological Effects. Inhibition of Cellular Proliferation. Rituximab inhibits the proliferation of Ramos, Daudi, and other NHL B-cells (10, 11). To examine whether the NF-κB pathway was involved in the proliferation, an aliquot of the cells (10^4 cells per sample) was used in a 24-hour standard XTT assay to analyze the cytostatic effects of rituximab and various NF-κB inhibitors. These inhibitors consisted of Bay 11-7085, an irreversible inhibitor of IκB-α phosphorylation that inhibits NF-κB DBA (28, 29); the cell-permeable inhibitory peptide SN50 that contains the nuclear localization signal of NF-κB (p50; ref. 30); and DHMEQ, a novel specific inhibitor of NF-κB nuclear translocation (32, 33). The results presented in Fig. 5*A* show that the NF-κB inhibitors inhibited the proliferation of both cell lines and mimic the cytostatic effect of rituximab, suggesting that the observed cytostasis of the Ramos and Daudi cells induced by rituximab might be through rituximab-mediated inhibition of the NF-κB pathway.

Chemosensitization. Based on the above findings, rituximab inhibits the NF-κB signaling pathway (Figs. 3 and 4) and sensitizes the cells to paclitaxel (Fig. 1). Thus, we examined whether the NF-κB pathway was involved in rituximab-mediated chemosensitization using NF-κB–specific inhibitors. Optimal concentrations of the inhibitors were determined by pilot studies and are in accordance with previous reports (28–30, 32, 33). The cells were pretreated with the inhibitors (Bay 11-7058, 4 μmol/L, 1 hour; DHMEQ, 10 μg/mL, 1 hour; SN50, 50 μg/mL, 3.5 hours) followed by paclitaxel (10 nmol/L, 18 hours). Paclitaxel alone induced modest apoptosis and the inhibitors at concentrations used were nontoxic to the cells. However, treatment of the cells with various NF-κB inhibitors sensitized the cells to paclitaxel (plus *cis*-diamminedichloroplatinum and etoposide; data not shown)–induced apoptosis. The extent of sensitization mimicked rituximab (Fig. 5*B*), suggesting that rituximab-mediated inhibition of the NF-κB signaling pathway may be involved in rituximab-mediated chemosensitization of tumor cells.

Rituximab-Mediated Up-Regulation of RKIP Expression and Inhibition of the NF-κB Signaling Pathway. The possible mechanism by which rituximab inhibits the NF-κB signaling pathway was examined. Recently, RKIP has been identified as a

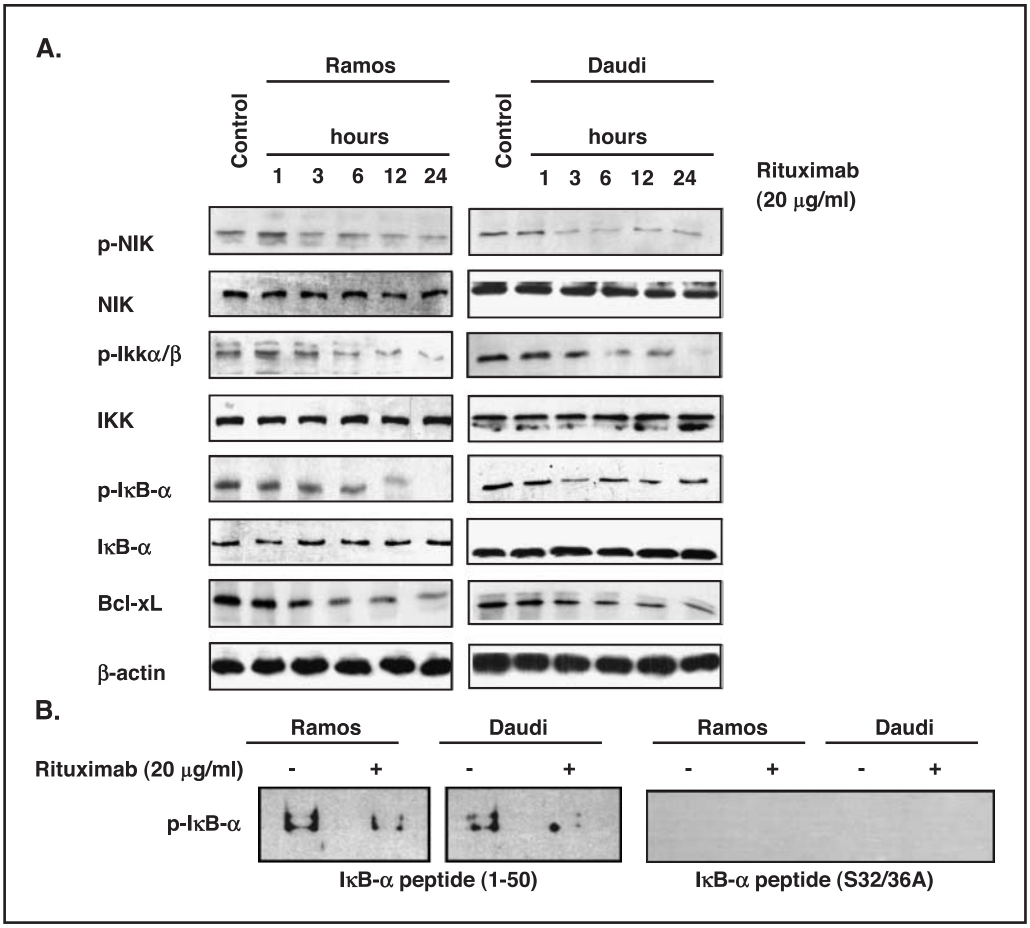

Figure 4. Rituximab inhibits the NF-κB signal transduction pathway. *A,* after overnight growth in RPMI 1640 + 1% fetal bovine serum, Ramos and Daudi cells were washed and grown in complete medium ± rituximab (20 μg/mL, 1-24 hours). Total cell lysates (40 μg) were subjected to Western blot analysis using phosphospecific and non-phosphospecific antibodies for various components of the NF-κB pathway. *B,* total cell lysates of the cells (±20 μg/mL rituximab, 24 hours) were subjected to immune complex kinase assay using IκB-α peptides (amino acids 1-50 $Ser^{32/36}$ and $Ser^{32/36A}$) as substrate. Representative of two independent experiments.

negative regulator of the NF-κB signaling pathway (25). Therefore, we examined if RKIP induction was associated with rituximab-mediated inhibition of the NF-κB pathway. We observed a time-dependent induction of RKIP in rituximab-treated Ramos cells as early as 3 to 6 hours post-treatment that remained at high levels up to 24 hours (Fig. 6*A* and *B*). Similar results were observed in Daudi cells (data not shown).

RKIP interrupts the NF-κB pathway via physical interaction with NIK, TAK1, and IKK (25); thus, we examined whether rituximab enhances the association between RKIP and these signaling molecules. Using specific antibodies, NIK, IKK, and TAK1 were precipitated from the total cell lysates of the tumor cells (with or without rituximab 20 μg/mL, 24 hours) and the membranes were subsequently immunoblotted with anti-RKIP polyclonal antibody. As depicted in Fig. 6*C*, the association of RKIP with NIK, TAK1, and IKK was significantly enhanced by rituximab. In addition, the lysates contained similar levels of these signaling molecules, whereas rituximab-treated cells exhibited higher levels of RKIP (Fig. 6*C*). Irrelevant antibody (Bcl-x_L), IgG, and beads were used as controls to show the specificity of the assay. These results show that rituximab up-regulates RKIP expression and augments its physical association with NIK, TAK1, and IKK, events that possibly account for rituximab-mediated inhibition of the NF-κB pathway.

Bcl-x_L Down-Regulation Is a Result of Rituximab-Mediated Inhibition of the NF-κB Pathway. The above findings show that rituximab inhibits the NF-κB pathway (Figs. 3 and 4) and Bcl-x_L expression (Figs. 2 and 4). Previous reports indicated that NF-κB partly regulates Bcl-x_L expression (20–23). Thus, we examined the direct relationship between inhibition of the NF-κB pathway and Bcl-x_L expression by rituximab. To this end, Ramos and Daudi B-cell lines with a functional block in the NF-κB signaling pathway were established. The strategy involved the overexpression of a chimeric fusion protein consisting of a dominant-active IκB-α mutant ($Ser^{32/36A}$) fused to a mutated ER ligand binding domain (44). The IκB mutant is incapable of being phosphorylated at the critical serine residues and thus is not targeted for proteasomal degradation on IKK activation. The fused ER confers inducible activation of the gene of interest on exposure to the synthetic estrogen 4-OHT. The FLAG-IκB-mutant-ER construct was cloned into the pcDNA3 expression vector and was stably transfected into the cells. Single clones expressing the construct were isolated and used for further analysis (21). The Ramos-IκB-ER and Daudi-IκB-ER cells were left either untreated or pretreated with 4-OHT (200 nmol/L, 8 hours). Then, the cell lysates were subjected to immunoblotting. As depicted, 4-OHT reduced the basal levels of Bcl-x_L in these cells (similar to rituximab), demonstrating that inhibition of NF-κB inhibits of Bcl-x_L expression (Fig. 7*A*).

Visual inspection of the sequence and computer database analysis revealed the presence of two-tandem, potential NF-κB consensus binding sites on the Bcl-x promoter located at positions −77 and −62 relative to transcription initiation site (data not shown). Thus, luciferase reporter assays were done to assess the ability of NF-κB to drive transcription from the Bcl-x promoter. To this end, a 650-bp DNA fragment spanning the Bcl-x 5′ promoter region (Bcl-x WT) and another reporter with an internal deletion spanning the potential NF-κB binding sites (Bcl-x ΔκB) were inserted into pGL2-Basic luciferase plasmids (21). Ramos and Daudi cells were transfected with these plasmids and the cells were allowed to recover for 36 hours. Thereafter, the cells were treated with either rituximab (20 μg/mL) or Bay 11-7085 (4 μmol/L) for another 18 hours. Then, the cells were harvested and the luciferase activity was measured. As shown, transfection with the WT promoter resulted in significant luciferase activity in both cell lines, albeit to varying degree. This difference is due to the differences in transfection efficiency of the cells. However, transfection of the cells with ΔκB promoter construct diminished the luciferase activity, an effect that was mimicked by rituximab and Bay 11-7085 (Fig. 7*B*). These results show that the presence of the two NF-κB sites in the upstream promoter region supports Bcl-x_L transcription, and this effect is abrogated either by deletion of the NF-κB binding sites or by rituximab and Bay 11-7085.

Because rituximab decreased both NF-κB DBA (Fig. 3) and Bcl-x_L expression (Figs. 2 and 4), we examined whether the NF-κB inhibitors modulate Bcl-x_L transcription similar to rituximab. Cells were either left untreated or treated with rituximab (20 μg/mL), Bay 11-7085 (4 μmol/L), SN50 (50 μg/mL), or DHMEQ (10 μg/mL), and total RNA was extracted and reverse transcribed to first-strand cDNA. Oligonucleotide primers specific for Bcl-x_L mRNA were used in a PCR reaction. NF-κB inhibitors decreased Bcl-x_L transcription and the inhibition was comparable with rituximab-mediated effect (Fig. 7*C*). The Bcl-2 family inhibitor, 2MAM-A3, which impairs the function of Bcl-x_L (31), did not affect the transcription of Bcl-x_L (Fig. 7*C*). Altogether, these results denote the involvement of NF-κB in the regulation of Bcl-x_L expression and the ability of rituximab to decrease NF-κB–dependent Bcl-x_L transcription.

Rituximab-Mediated Bcl-x_L Down-Regulation Is Responsible for Chemosensitization of Tumor Cell. The above findings show that rituximab-mediated inhibition of the NF-κB pathway is partially responsible for Bcl-x_L down-regulation. In addition, rituximab chemosensitized the cells. To confirm the protective role of Bcl-x_L in paclitaxel-induced apoptosis, parental Ramos and Daudi cells were grown either in complete medium or in complete medium supplemented with 2MAM-A3 (15 and 20 μg/mL, 7 hours) followed by paclitaxel (10 nmol/L, 18 hours) treatment. As shown, 2MAM-A3 by itself was inefficient in killing the tumor cells but significantly augmented paclitaxel (*cis*-diamminedichloroplatinum and etoposide; data not shown)–induced apoptosis in both cell lines, albeit to varying degrees (Fig. 8*A*).

Additionally, the stable transfectants Ramos-IκB-ER and Daudi-IκB-ER with or without 4-OHT (10^6 cells/mL) were treated with paclitaxel (10 nmol/L, 18 hours). 4-OHT, which lowers Bcl-x_L levels (Fig. 7*A*), sensitized the cells to paclitaxel at levels comparable with those achieved by rituximab (Fig. 8*B*). These results suggest that an intact NF-κB signaling pathway is required for the maintenance of the drug resistance phenotype, and disruption of this pathway using IκB superrepressor construct, which diminishes Bcl-x_L levels, renders the cells chemosensitive.

To further ascertain the protective role of Bcl-x_L against drug-induced apoptosis, Ramos cells were stably transfected with hemagglutinin-tagged Bcl-x_L–expressing construct (21), which migrates slightly slower than the endogenous Bcl-x_L, allowing for comparative analysis of expression levels on treatment. The expression levels of endogenous and ectopically expressed Bcl-x_L compared with the parental cell line was confirmed (Fig. 8*C*, *1*) and the HA-Bcl-x_L cells exhibited higher resistance to paclitaxel (*cis*-diamminedichloroplatinum, etoposide, and Adriamycin; data not shown) compared with the parental cell line. Rituximab

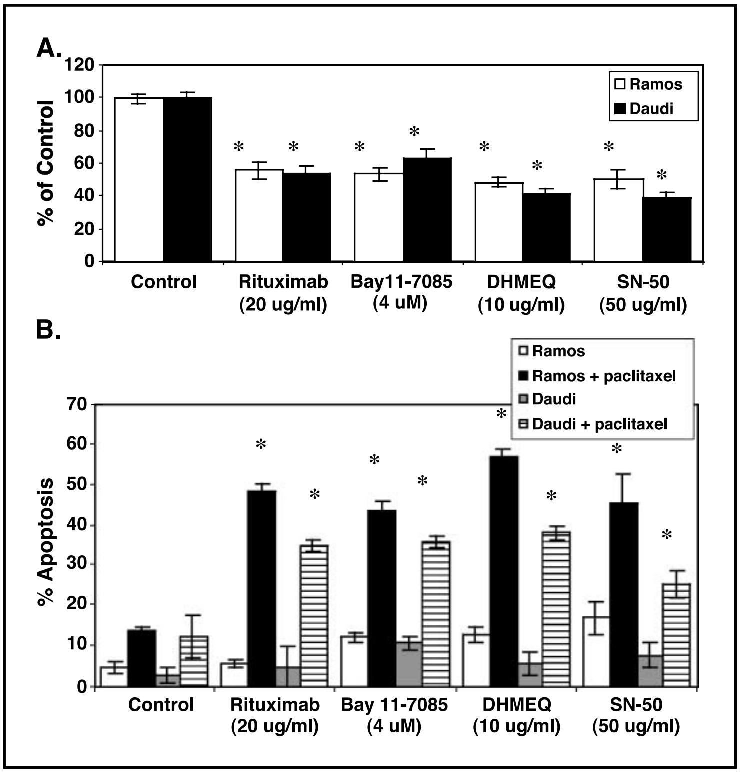

Figure 5. Pharmacologic inhibition of the NF-κB signal transduction pathway. *A,* inhibition of proliferation of the Ramos and Daudi cells by rituximab and the NF-κB inhibitors. Tumor cells were left either untreated or pretreated with rituximab (20 μg/mL), Bay 11-7085 (4 μmol/L), DHMEQ (10 μg/mL), or SN50 (50 μg/mL); 10^4 cells per sample were used in a 24-hour XTT assay. *B,* chemosensitization: cells were left eitheruntreated or pretreated with rituximab (20 μg/mL, 24 hours), Bay 11-7085 (4 μmol/L, 1 hour), DHMEQ (10 μg/mL, 1 hour), or SN50 (50 μg/mL, 3.5 hours). Cells (2×10^6) were then incubated with paclitaxel (10 nmol/L, 18 hours) and subjected to PI staining. Samples were set up in triplicates. *Columns,* mean of two independent experiments; *bars,* SD. *, $P < 0.05$, compared with control (*A*) or paclitaxel treatment (*B*) alone.

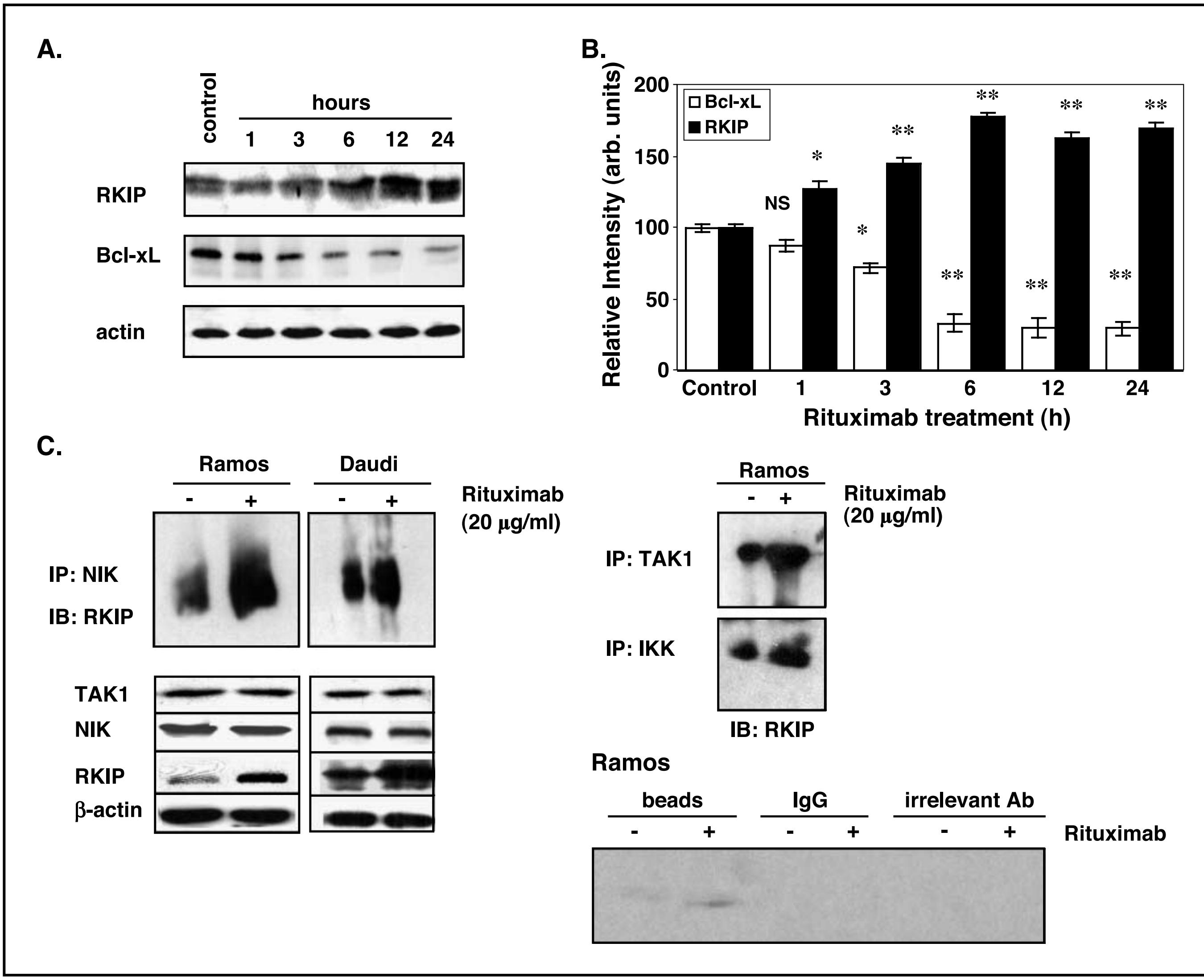

Figure 6. Rituximab induces RKIP expression and augments its physical association with endogenous NIK, TAK1, and IKK. *A,* Ramos cells were grown in complete medium ± rituximab (20 μg/mL, 1-24 hours) and total cell lysates (40 μg) were subjected to immunoblot analysis. *B,* densitometric analysis: an inverse correlation between RKIP and Bcl-x_L expression on exposure to rituximab. *Columns,* mean ($n = 2$); *bars,* SD. *C,* immunoprecipitation of RKIP: endogenous NIK, TAK1, and IKK were immunoprecipitated and the membranes were blotted with anti-RKIP antibody. Representative of two independent experiments. *, $P < 0.05$, compared with control.

reduced endogenous Bcl-x_L levels (Fig. 8*C*, *1*) and was not as efficient in sensitizing these cells to paclitaxel-induced apoptosis compared with the parental cells (Fig. 8*C*, *2*). However, higher concentrations of 2MAM-A3 (35 μg/mL) and paclitaxel (20 nmol/L) were needed to kill the HA-Bcl-x_L Ramos cells (Fig. 8*C*, *3*) compared with the low concentrations required for the killing of the parental cells (2MAM-A3 15 and 20 μg/mL; paclitaxel 10 nmol/L).

Discussion

This study provides evidence for the first time that rituximab treatment of NHL B-cell lines inhibits the constitutive NF-κB signaling pathway via up-regulation of RKIP expression. These effects result in down-regulation of Bcl-x_L expression and chemosensitization of the tumor cells. We show that rituximab inhibits the NF-κB signaling pathway by decreasing the phosphorylation-dependent state of the components of this pathway and inhibition of IKK kinase activity concomitant with up-regulation of RKIP expression. Induction of RKIP augments its physical association with endogenous NIK, TAK1, and IKK, resulting in decreased activity of the NF-κB pathway and diminished NF-κB DBA. Inhibition of NF-κB activity resulted in down-regulation of Bcl-x_L and Bfl-1/A1 expression and subsequent chemosensitization of the NHL B-cell lines. Rituximab-mediated Bcl-x_L down-regulation via inhibition of the NF-κB signaling pathway was corroborated by the use of NF-κB–specific inhibitors. The direct role of NF-κB in rituximab-mediated chemosensitization was shown by functional block of the NF-κB pathway using cell lines stably transfected with IκB-α superrepressor (incapable of being phosphorylated), and these cell lines were sensitive to drug-induced apoptosis in the absence of rituximab. The presence of two-tandem NF-κB binding sites in the upstream promoter region of the *Bcl-x* gene supported the role of NF-κB in the regulation of Bcl-x_L expression, which was diminished by the deletion of the NF-κB binding sites similar to rituximab. The pivotal role of Bcl-x_L in chemoresistance was confirmed using Bcl-x_L–overexpressing cells, which exhibited higher drug resistance and were minimally sensitized by rituximab or a Bcl-x_L–specific inhibitor. The involvement of the NF-κB signaling pathway in the proliferation of NHL cells was confirmed by using NF-κB–specific inhibitors, which reduced the proliferation rate to the levels achieved by rituximab, suggesting a link between rituximab-mediated cytostasis and inhibition of the

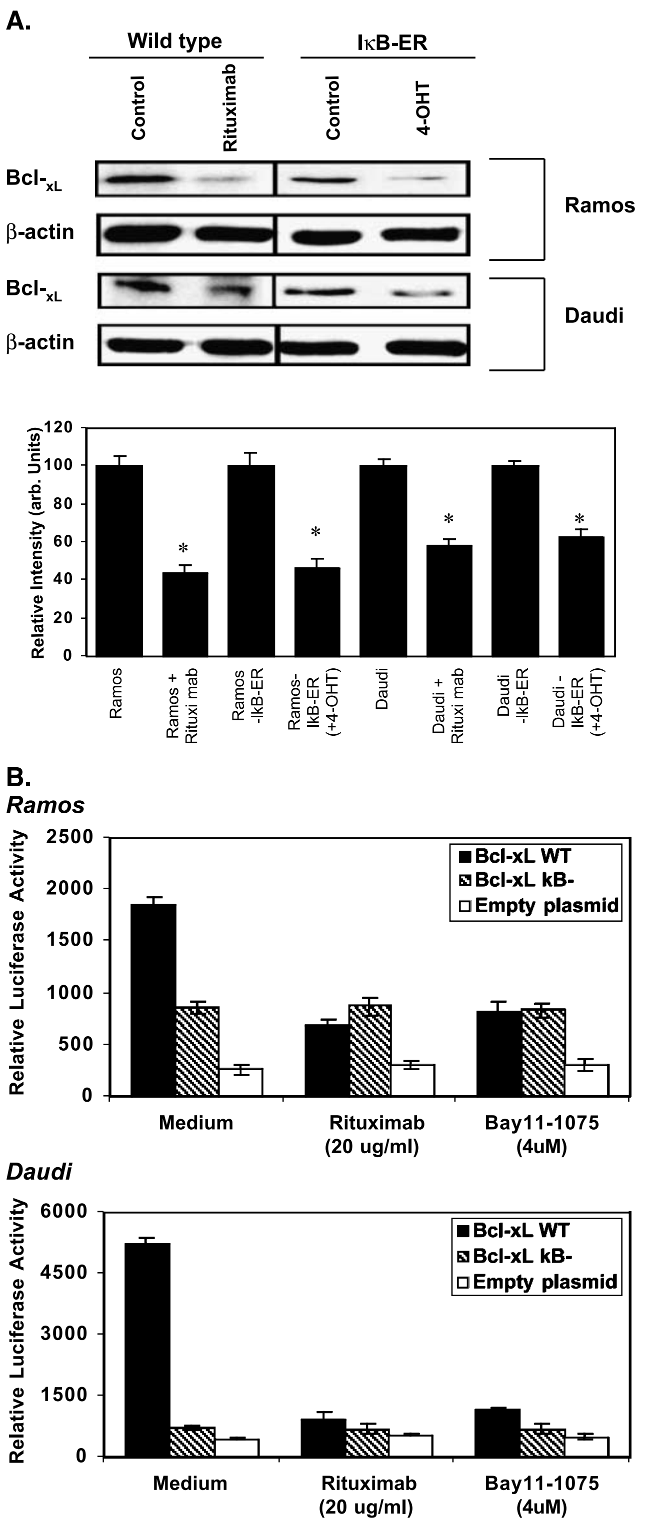

Figure 7. An intact NF-κB signal transduction pathway is required for Bcl-x_L expression. *A,* total cell lysates (40 μg) of the Ramos-IκB-ER and Daudi-IκB-ER cells ± 4-OHT (200 nmol/L, 8 hours) were subjected to immunoblotting for Bcl-x_L expression. *B,* a Bcl-x promoter fragment spanning −640 to +9 region relative to the transcriptional start site (Bcl-x WT) and another fragment lacking two-tandem NF-κB binding sites (Bcl-x ΔκB) were cloned into the pGL2-Basic luciferase reporter vector (21). Ramos and Daudi cells were then transfected with 10 μg of the indicated reporter plasmids or empty vector. Thirty-six hours post-transfection, the cells were left either untreated or treated with Bay 11-7085 (4 μmol/L) or rituximab (20 μg/mL), harvested after 18 hours, and assessed for luciferase activity. *C,* total RNA of WT Ramos and Daudi ± 2MAM-A3 (20 μg/mL), rituximab (20 μg/mL), SN50 (50 μg/mL), DHMEQ (10 μg/mL), or Bay 11-7085 (4 μmol/L) was reverse transcribed to first-strand cDNA; 2.5 μg of each cDNA were used in PCR analysis. Intensity of the bands was normalized to the levels of the corresponding β-actin or glyceraldehyde 3-phosphate dehydrogenase. Representative of two independent experiments. *, $P < 0.05$, compared with control.

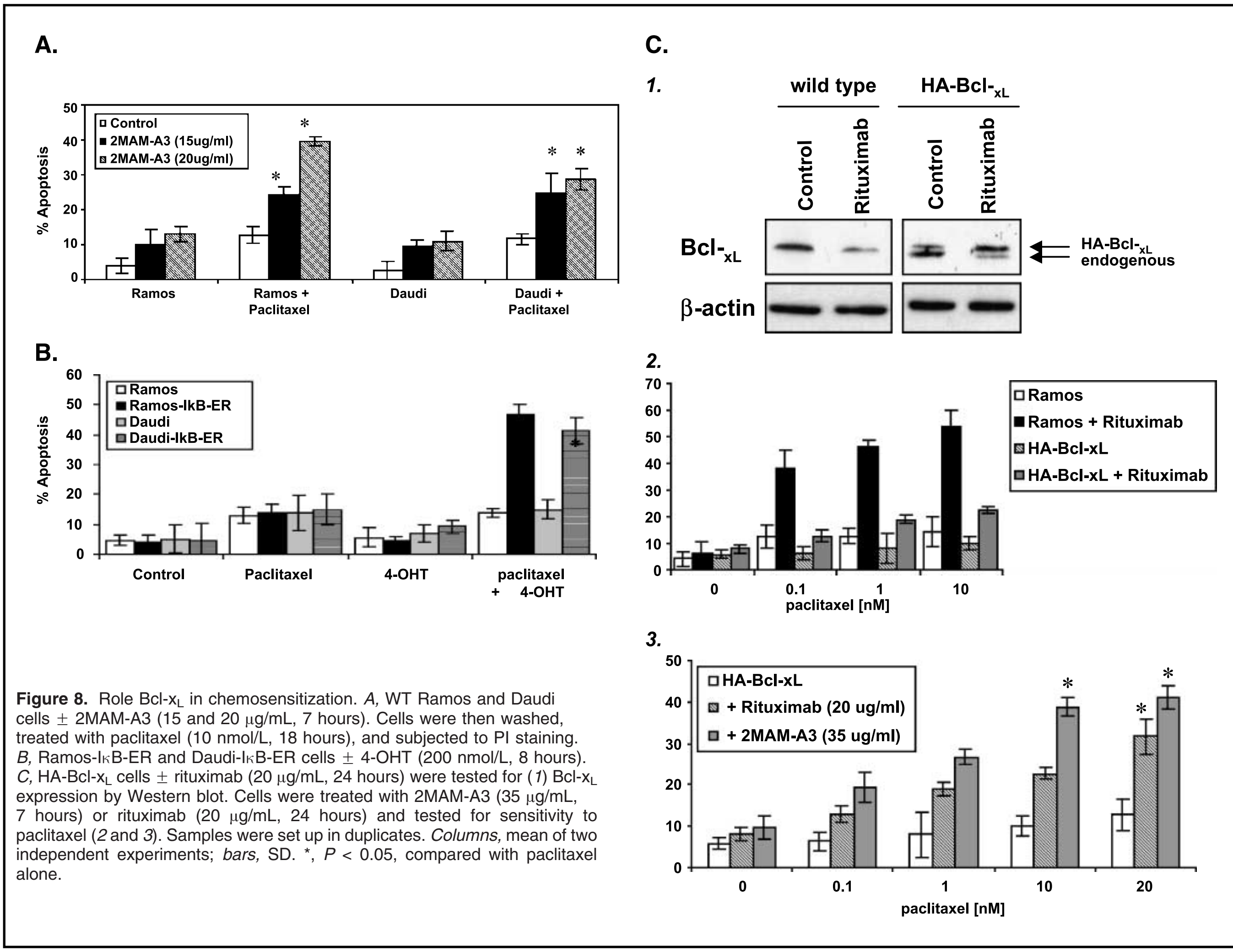

Figure 8. Role Bcl-x_L in chemosensitization. *A,* WT Ramos and Daudi cells ± 2MAM-A3 (15 and 20 μg/mL, 7 hours). Cells were then washed, treated with paclitaxel (10 nmol/L, 18 hours), and subjected to PI staining. *B,* Ramos-IκB-ER and Daudi-IκB-ER cells ± 4-OHT (200 nmol/L, 8 hours). *C,* HA-Bcl-x_L cells ± rituximab (20 μg/mL, 24 hours) were tested for (*1*) Bcl-x_L expression by Western blot. Cells were treated with 2MAM-A3 (35 μg/mL, 7 hours) or rituximab (20 μg/mL, 24 hours) and tested for sensitivity to paclitaxel (*2* and *3*). Samples were set up in duplicates. *Columns,* mean of two independent experiments; *bars,* SD. *, $P < 0.05$, compared with paclitaxel alone.

NF-κB signaling pathway. These results provide a rational molecular mechanism underlying the synergy achieved by the combination of rituximab and drugs.

Constitutive activation of the NF-κB/Rel transcription factors has been observed in various malignancies including B-cell lymphoma (45). Likewise, the NF-κB pathway is constitutively activated in Ramos and Daudi cells (Figs. 3 and 4). Constitutive activation of NF-κB/Rel either through the amplification of *Rel* genes or through aberrant activation of the upstream regulators contributes to pathologic conditions including cancer (17–19). In mammals, the NF-κB family contains five members: RelA (p65), RelB, c-Rel, NF-κB1 (p50 and its precursor p105), and NF-κB2 (p52 and its precursor p100), the most abundant form being the p65/p50 heterodimer. In normal cells, NF-κB activity is tightly controlled by IκB inhibitory proteins. NF-κB activation can be induced by a plethora of extracellular stimuli resulting in phosphorylation of IκB at two conserved serines in the NH_2-terminal regulatory region, which in IκB-α correspond to $Ser^{32/36}$. This phosphorylation step is rapidly followed by polyubiquitination and IκB degradation by the 26S proteosome, allowing stable translocation of NF-κB to the nucleus and activation of gene transcription. IκB phosphorylation is catalyzed by the multiprotein IKK complex, which is phosphorylated and activated by the upstream NIK (17–19). Herein, we show a significant decrease in the phosphorylation-dependent state of NIK, IKK, and IκB-α as well as the DBA of NF-κB 3 to 6 hours post-rituximab treatment in NHL B-cells concomitant with diminished enzymatic activity of IKK (Figs. 3 and 4) suggestive of a novel function for rituximab as a negative regulator of the NF-κB pathway. The inhibition of the NF-κB pathway by rituximab was not complete, as mechanisms other than NIK/IKK/IκB might be implicated in the residual activity of the NF-κB signaling pathway (46).

The inhibition of the NF-κB pathway might occur via several different mechanisms (46, 47). Recently, modulation of RKIP expression is reported as a novel mechanism of NF-κB inhibition (25). *In vitro*, RKIP disrupts the interaction between NIK and IKK, thus behaving as a competitive inhibitor for IKK. Physical association between RKIP and endogenous TAK1, NIK, and IKK will abrogate the ability of these signaling molecules to phosphorylate and activate downstream molecules and, by suppressing the NF-κB pathway, decreases NF-κB dependent gene expression (25). Our findings reveal that rituximab up-regulates the expression of RKIP and augments its physical association with three major signaling molecules involved in NF-κB signal transduction pathways (Fig. 6), thus reducing the phosphorylation of the components of the NF-κB pathway and the NF-κB DBA, all of which occur with similar time kinetics culminating in reduced IKK kinase activity.

The NF-κB/Rel transcription factors bind to κB control elements present in the promoter of a wide variety of target genes that regulate cellular differentiation, proliferation, survival, and apoptosis (17–19). Activation of the NF-κB pathway by various stimuli is, in part, responsible for the transcriptional activation and expression of antiapoptotic Bcl-2 and inhibitors of apoptosis protein family members, which rescue tumor cells from drug-induced apoptosis (17–24, 47). Herein, we show that rituximab inhibits the NF-κB signaling pathway resulting in down-regulation of Bcl-x_L and Bfl-1/A1. The basal levels of Bfl-1/A1 were substantially lower compared with Bcl-x_L. Bcl-x_L is highly expressed in follicular lymphoma (13) and we have recently reported that inhibition of Bcl-x_L expression is critical for rituximab-mediated chemosensitization of NHL cells (11, 48). Thus, we examined the direct involvement of the NF-κB signaling pathway in Bcl-x_L expression by various approaches. First, using Ramos and Daudi cell lines expressing a superrepressor, dominant-active IκB (IκB-ER), we established that an intact NF-κB signaling pathway is essential for Bcl-x_L expression (Fig. 7*A*). Second, promoter reporter assays showed that NF-κB drives the expression of Bcl-x_L, and deletion of NF-κB binding sites in the upstream promoter region mimicked rituximab-mediated and Bay 11-7085–mediated effects in reducing luciferase activity (Fig. 7*B*). Third, the role of NF-κB in Bcl-x_L expression was corroborated by pharmacologic interruption of the NF-κB pathway using specific inhibitors, which reduced Bcl-x_L expression at levels comparable with those achieved by rituximab (Fig. 7*C*). Whereas this study shows that NF-κB regulates, in part, Bcl-x_L expression, detailed analysis of the Bcl-x promoter reveals consensus binding sites for several other transcription factors including Ets, signal transducers and activators of transcription, and activator protein-1 (23). Indeed, our preliminary findings suggest the partial involvement of the extracellular signal-regulated kinase-1/2 pathway and activator protein-1 in the regulation of Bcl-x_L expression in NHL B-cells (48).

Our results suggest that, in Bcl-2–deficient Ramos and Bcl-2-expressing Daudi cells, Bcl-x_L is the main antiapoptotic factor and the ability of rituximab to negatively modulate the expression of Bcl-x_L may explain rituximab effectiveness in combination with chemotherapy in reversing drug resistance. The protective role of Bcl-x_L against chemotherapy-triggered apoptosis (12, 15, 16) was supported by using Bcl-x_L–overexpressing cells, which expressed higher resistance against a battery of structurally and functionally unrelated drugs (paclitaxel, *cis*-diamminedichloroplatinum, Adriamycin, and etoposide; data not shown). The involvement of Bcl-x_L was also confirmed by treatment of IκB superrepressor cells with 4-OHT (which reduced Bcl-x_L levels; Fig. 7*A*) that exhibited higher sensitivity to paclitaxel-induced apoptosis (Fig. 8*B*). Furthermore, 2MAM-A3, which binds to Bcl-x_L at the hydrophobic groove formed by the highly conserved BH1, BH2, and BH3 domains, thus impairing the antiapoptotic ability of Bcl-x_L, was used (31). Although unable to regulate transcription or translation of Bcl-x_L, higher concentrations of 2MAM-A3 were required to sensitize the Bcl-x_L–overexpressing Ramos (Fig. 8*C*, *3*). Our findings with Bcl-2-expressing Daudi and Bcl-2–deficient Ramos cells suggest that rituximab-mediated chemosensitization may be independent of Bcl-2 expression, which is in agreement with recent findings (49).

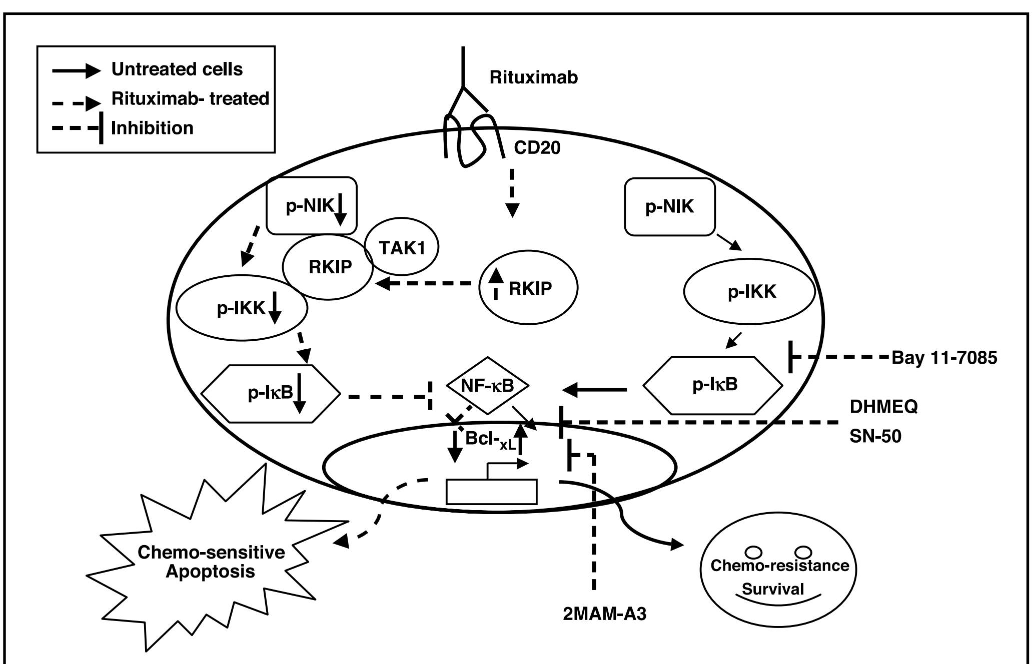

Figure 9. Proposed model of rituximab-mediated inhibition of the NF-κB pathway and chemosensitization of NHL B-cells. NF-κB signaling pathway is constitutively active in Ramos and Daudi cells and these cells express low levels of RKIP. On ligation to CD20, rituximab up-regulates RKIP expression. RKIP blocks the phosphorylation and activation of NIK, TAK1, and IKK via physical association and renders them incapable of relaying the signal to the downstream components of the signaling cascade. This will in turn result in decrease in the phosphorylation-dependent state of IKK and IκB-α and inhibition of the activity of the NF-κB pathway. Subsequently, the DBA of the transcription factor NF-κB is diminished culminating in decreased NF-κB-dependent gene expression. Deactivation of the NF-κB pathway will (*A*) decrease the proliferation rate of the tumor cells, (*B*) diminish the levels of Bcl-x_L and Bfl-1/A1, which will decrease the apoptosis threshold, and (*C*) chemosensitize the NHL B-cells. Pharmacologic inhibition of the NF-κB pathway (by Bay 11-7085, DHMEQ, and SN50), functional block of NF-κB (by IκB superrepressor cells), or functional impairment of Bcl-x_L (by 2MAM-A3) mimics the antiproliferative and chemosensitizing effects of rituximab.

Activation of NF-κB is emerging as one of the major mechanisms of tumor cell resistance to drugs (17–24). Thus, interruption of this pathway is a target for therapeutic intervention for the treatment of tumors (50, 51), which has proven successful in enhancing the apoptotic effects of anticancer agents (e.g., tumor necrosis factor-α and CPT-11) resulting in tumor regression *in vivo* (52). Bcl-x_L is a downstream target of the NF-κB pathway (20–23); rescues tumor cells from drug cytotoxicity (17–24, 47); is abundantly expressed in lymphomas (13, 53); antagonizes DNA-damaging agents and metabolic, microtubule, and topoisomerase inhibitors; and through modulation of apoptosis plays a major role in the determination of cellular response to a wide variety of apoptosis-inducing stimuli (12–16, 52), which can be considered as prognostic markers in lymphoma (13, 53). Targeted suppression of Bcl-x_L expression facilitated drug-induced B-cell leukemia tumor regression in SCID/NOD-Hu *in vivo* model (54). Our results corroborate previous reports where inhibition of NF-κB, Bcl-x_L, and Bfl-1/A1 augmented drug-induced, Fas-induced, and tumor necrosis factor-α–induced apoptosis in various systems (21, 22, 24, 47). Our results also show that rituximab-mediated RKIP expression inhibits the NF-κB signaling pathway concomitant with Bcl-x_L down-regulation resulting in chemosensitization of tumor cells. The regulation of RKIP expression by rituximab is currently under investigation. Induction of RKIP on apoptotic stimuli is also observed in prostate cancer cells. Enforced overexpression of RKIP in the drug-resistant tumor cells has a chemosensitizing effect and its down-regulation confers resistance to chemotherapeutic agents (55). Thus, RKIP might represent a novel apoptotic marker, and its role in the regulation of cell survival and apoptosis in cancer cells may be of significant clinical relevance (56). Further, a novel antimetastatic function for RKIP in prostate and melanoma cancer has recently been proposed (57, 58).

In conclusion, we have described a novel signaling pathway triggered by rituximab schematically shown in Fig. 9. Rituximab up-regulates RKIP expression, which negatively affects the NF-κB survival signaling pathway. This diminishes NF-κB DBA and NF-κB–dependent expression of antiapoptosis gene products and then decreases the apoptosis threshold and chemosensitizes the cells through the type II mitochondrial apoptotic pathway (11). Functional block of NF-κB (e.g., IκB mutant cells), pharmacologic interruption of the NF-κB pathway (e.g., Bay 11-7085, DHMEQ, and SN50), or functional impairment of Bcl-x_L (e.g., 2MAM-A3) can mimic, in part, the antiproliferative and chemosensitizing effects of rituximab. Hence, this study identifies several potential targets for therapeutic intervention (i.e., the components of the NF-κB pathway and RKIP) and provides a rational molecular basis for the use of rituximab and/or the NF-κB pharmacologic inhibitors alone or in combination with subtoxic concentrations of chemotherapeutic drugs in rituximab/drug refractory NHL.

Acknowledgments

Received 6/10/2004; revised 8/31/2004; accepted 10/20/2004.

Grant support: Jonsson Comprehensive Cancer Center, University of California at Los Angeles (A.R. Jazirehi) and UC-MEXUS Conacyt fellowship (S. Huerta-Yepez).

The costs of publication of this article were defrayed in part by the payment of page charges. This article must therefore be hereby marked advertisement in accordance with 18 U.S.C. Section 1734 solely to indicate this fact.

We thank Drs. Mario Vega, Paul Dempesy, Alex Cheng, and Brian Zarnegar for valuable insights, technical support, and reagents; Dr. Kazuo Umezawa (Tokyo, Japan) for providing DHMEQ; Drs. Devasis Chatterjee and Lee Goodglick for helpful discussions; and Christine Yue for the preparation of the article.

References

1. Swerdlow AJ. Epidemiology of Hodgkin's disease and non-Hodgkin's lymphoma. Eur J Nucl Med Mol Imaging 2003;30:S3–12.

2. Coffey J, Hodgson DC, Gospodarowicz MK. Therapy of non-Hodgkin's lymphoma. Eur J Nucl Med Mol Imaging 2003;30:S28–36.

3. Theodossiou C, Schwarzenberger P. Non-Hodgkin's lymphomas. Clin Obstet Gynecol 2002;45:820–9.

4. Einfeld DA, Brown JP, Valentine MA, Clark EA, Ledbetter JA. Molecular cloning of the human B cell CD20 receptor predicts a hydrophobic protein with multiple transmembrane domains. EMBO J 1988;7:711–7.

5. Press OW, Applebaum F, Ledbetter JA. Monoclonal 1F5 (anti-CD20) serotherapy of human B cell lymphomas. Blood 1987;69:584–91.

6. Reff ME, Carner K, Chambers KS, et al. Depletion of B cells *in vivo* by a chimeric mouse human monoclonal antibody to CD20. Blood 1994;83:435–45.

7. Czuczman MS, Fallon A, Mohr A, et al. Rituximab in combination with CHOP or fludarabine in low-grade lymphoma. Semin Oncol 2002;29:36–40.

8. Coiffier B. Immunochemotherapy: the new standard in aggressive non-Hodgkin's lymphoma in the elderly. Semin Oncol 2003;30:21–7.

9. Maloney DG, Smith B, Rose A. Rituximab: mechanism of action and resistance. Semin Oncol 2002;29:2–9.

10. Alas S, Bonavida B. Rituximab inactivates STAT3 activity in B-non-Hodgkin's lymphoma through inhibition of the interleukin 10 autocrine/paracrine loop and results in down-regulation of Bcl-2 and sensitization to cytotoxic drugs. Cancer Res 2001;61:5137–44.

11. Jazirehi AR, Gan XH, de Vos S, Emmanouilides C, Bonavida B. Rituximab (anti-CD20) selectively modifies Bcl-$_{xL}$ and Apaf-1 expression and sensitizes human non-Hodgkin's lymphoma B cell lines to paclitaxel-induced apoptosis. Mol Cancer Ther 2003;2:1183–93.

12. Tudor G, Aguilera A, Halverson DO, Laing ND, Sauville EA. Susceptibility to drug-induced apoptosis correlates with differential modulation of Bad, Bcl-2 and Bcl-$_{xL}$ protein levels. Cell Death Differ 2000;7:574–86.

13. Xerri L, Parc P, Brousset P, et al. Predominant expression of the long isoform of Bcl-x (Bcl-$_{xL}$) in human lymphomas. Br J Haematol 1996;92:900–6.

14. Reed JC. Bcl-2 family proteins: regulators of chemoresistance in cancer. Toxicol Lett 1995;82:155–8.

15. Minn AJ, Rudin CM, Boise LH, Thompson CB. Expression of Bcl-$_{xL}$ can confer a multi-drug resistance phenotype. Blood 1995;86:1903–10.

16. Amundson SA, Myers TG, Scudiero D, Kitada S, Reed JC, Fornace A Jr. An informatics approach identifying markers of chemosensitivity in human cancer cell lines. Cancer Res 2000;60:6101–10.

17. Ghosh S, Karin M. Missing pieces in the NF-κB puzzle. Cell 2002;109:S81–96.

18. Dixit V, Mak TW. NF-κB signaling: many roads lead to Madrid. Cell 2002;111:615–9.

19. Karin M, Lin A. NF-κB at the crossroads of life and death. Nat Immunol 2002;3:221–7.

20. Chen C, Edelstein LC, Gelinas C. The Rel/NF-κB family directly activates expression of the apoptosis inhibitor Bcl-xl. Mol Cell Biol 2000;20:2687–95.

21. Lee HH, Dadgostar H, Cheng Q, Shu J, Cheng G. NF-κB-mediated up-regulation of Bcl-x and Bfl-1/A1 is required for CD40 survival signaling in B lymphocytes. Proc Natl Acad Sci U S A 1999;96:9136–41.

22. Chen Q, Lee HH, Li Y, Parks TP, Cheng G. Upregulation of Bcl-x and Bfl-1 as a potential mechanism of chemoresistance, which can be overcome by NF-κB inhibition. Oncogene 2000;19:4936–40.

23. Sevilla L, Zaldumbide A, Pognonec P, Boulukos KE. Transcriptional regulation of the bcl-x gene encoding the anti-apoptotic Bcl-$_{xL}$ protein by Ets, Rel/NF-κB, STAT and AP-1 transcription factor families. Histol Histopathol 2001;16:595–601.

24. Manna SK, Haridus V, Aggrawal BB. Bcl-$_{xL}$ suppresses TNF-mediated apoptosis and activation of nuclear factor-κB, activation protein-1 and c-Jun N-terminal kinase. J Interferon Cytokine Res 2000;20:725–35.

25. Yeung KC, Rose DW, Dhillon AS, et al. Raf kinase inhibitor protein interacts with NF-κB-inducing kinase and TAK1 and inhibits NF-κB activation. Mol Cell Biol 2001;21:7207–17.

26. Klein E, Klein G, Nadkarni JS, Nadkarni JJ, Wigzell H, Clifford P. Surface IgM-κ specificity on a Burkitt lymphoma cell *in vivo* and in derived culture lines. Cancer Res 1968;28:1300–10.

27. Pierce JW, Schoenleber R, Jesmok G, et al. Novel inhibitors of cytokine induced IκB-α phosphorylation and endothelial cell adhesion molecule expression show anti-inflammatory effects *in vivo*. J Biol Chem 1997;272:21096–101.

28. Mori N, Yamada Y, Ikeda S, et al. Bay 11-7082 inhibits transcription factor NF-κB and induces apoptosis of HTLV-I-infected T-cell lines and primary adult T-cell leukemia cells. Blood 2002;100:1828–34.

29. Keller SA, Schattner EJ, Cesarman E. Inhibition of NF-κB induces apoptosis of KSHV-infected primary effusion lymphoma cells. Blood 2000;96:2537–42.

30. Lin YZ, Yao S, Veach RA, Torgerson TR, Hawiger J. Inhibition of nuclear translocation of transcription factor NF-κB by a synthetic peptide containing a cell membrane-permeable motif and nuclear localization sequence. J Biol Chem 1995;270:14255–8.

31. Tzung SP, Kim CM, Basanez G, et al. Antimycin A mimics a cell death-inducing Bcl-2 homology domain 3. Nat Cell Biol 2001;3:183–91.

32. Ariga A, Namekawa J, Matsumoto N, Inoue J, Umezawa K. Inhibition of tumor necrosis factor-α-induced nuclear translocation and activation of NF-κB by dehydroxymethylepoxyquinomicin. J Biol Chem 2002;277:24626–30.

33. Kikuchi E, Horiguhi Y, Nakashima J, et al. Suppression of hormone-refractory prostate cancer by a novel

nuclear factor κB inhibitor in nude mice. Cancer Res 2003;63:107–10.
34. Jazirehi AR, Ng CP, Gan XH, Schiller G, Bonavida B. Adriamycin sensitized the Adriamycin-resistant 8226/Dox40 human multiple myeloma cells to Apo2L/TRAIL-mediated apoptosis. Clin Cancer Res 2001;7:3874–83.
35. Jazirehi AR, Bonavida B. Resveratrol modifies the expression of apoptotic regulatory gene products and sensitizes non-Hodgkin's lymphoma and multiple myeloma cells to paclitaxel-induced apoptosis. Mol Cancer Ther 2004;3:71–84.
36. Lindmark R, Thoren-Tolling K, Sjoquist J. Binding of immunoglobulins to protein A and immuno-globulin levels in mammalian sera. J Immunol Methods 1983;62:1–13.
37. Nicoletti IG, Migliorati MC, Pagliacci F, Grignani C, Riccardi C. A rapid and simple method for measuring thymocyte apoptosis by propidium iodide staining and flow cytometry. J Immunol Methods 1991;139:271–9.
38. Scudiero DA, Shoemaker RH, Paull KD, et al. Evaluation of a soluble tetrazolium/formazan assay for cell growth and drug sensitivity using human and other tumor cell lines. Cancer Res 1988;48:4827–33.
39. Harada H, Takahashi EI, Itoh S, Harada K, Hori TA, Taniguchi T. Structure and regulation of the human interferon regulatory factor 1 (IRF-1) and IRF-2 genes: implications for a network in the interferon system. Mol Cell Biol 1994;14:1500–9.
40. Chou Q, Russell M, Birch DE, Raymond J, Bloch W. Prevention of pre-PCR mis-priming and primer dimerization improves low-copy-number amplifications. Nucleic Acids Res 1992;20:1717–23.
41. Dudley DT, Pang L, Decker SJ, Bridges AJ, Saltiel AR. A synthetic inhibitor of the mitogen-activated protein kinase cascade. Proc Natl Acad Sci U S A 1995;92:7686–9.
42. Berinstein NL, Grillo-Lopez AJ, White CA, et al. Association of serum Rituximab (IDEC-C2B8) concentration and anti-tumor response in the treatment of recurrent low-grade or follicular non-Hodgkin's lymphoma. Ann Oncol 1998;9:995–1001.
43. Shan D, Ledbetter JA, Press OW. Signaling events involved in anti-CD20-induced apoptosis of malignant human B cells. Cancer Immunol Immunother 2000;48:673–83.
44. Littlewood TD, Hancock DC, Danielian PS, Parker MG, Evan GI. A modified estrogen receptor ligand-binding domain as an improved switch for the regulation of heterologous proteins. Nucleic Acids Res 1995;23:1686–90.
45. Gilmore TD, Kalaitzidis D, Liang MC, Starczynowski DT. The c-Rel transcription factor and B-cell proliferation: a deal with the devil. Oncogene 2004;23:2275–86.
46. Kucharczak J, Simmons MJ, Fan Y, Gélinas C. To be, or not to be: NF-κB is the answer—role of Rel/NF-κB in the regulation of apoptosis. Oncogene 2003;22:8961–82.
47. Fujioka S, Sclabas GM, Schmidt ZC, et al. Inhibition of constitutive NF-κB activity by IκBαM suppresses tumorigenesis. Oncogene 2003;22:1365–70.
48. Jazirehi AR, Vega M, Chatterjee D, Goodglick L, Bonavida B. Inhibition of the Raf1-MEK1/2-ERK1/2 signaling pathway, Bcl-$_{xL}$ down-regulation and chemo-sensitization of non-Hodgkin's lymphoma (NHL) B-cells by rituximab. Cancer Res 2004;64:7117–26.
49. Claude Chan HT, Hughes D, French RR, et al. CD20-induced lymphoma cell death is independent of both caspases and its redistribution into Triton X-100 insoluble membrane rafts. Cancer Res 2003;63:5480–9.
50. Grag A, Aggarwal B. Nuclear transcription factor-κB as a target for cancer drug development. Leukemia 2002;16:1053–68.
51. Orlowski RZ, Baldwin AS Jr. NF-κB as a therapeutic target in cancer. Trends Mol Med 2002;8:385–9.
52. Wang, CU, Cusack JC Jr, Liu R, Baldwin AS Jr. Control of inducible chemo-resistance: enhanced anti-tumor therapy through increased apoptosis by inhibition of NF-κB. Nat Med 1999;5:412–7.
53. Zhao WL, Daneshpouy ME, Mounier N, et al. Prognostic significance of bcl-$_{xL}$ gene expression and apoptotic cell counts in follicular lymphoma. Blood 2004;103:695–7.
54. Fennell DA, Corbo MV, Dean NM, Monia BP, Cotter FE. *In vivo* suppression of Bcl-$_{xL}$ expression facilitates chemotherapy-induced leukemia cell death in a SCID/NOD-Hu model. Br J Hematology 2001;112:706–13.
55. Chatterjee D, Bai Y, Wang Z, et al. RKIP sensitizes prostate and breast cancer cells to drug-induced apoptosis. J Biol Chem 2004;279:17515–23.
56. Odabaie G, Chatterjee D, Jazirehi A, Goodglick L, Yeung K, Bonavida B. Raf kinase inhibitor (RKIP): structure, function, regulation of cell signaling and apoptosis. Adv Cancer Res 2004;91:169–200.
57. Fu Z, Smith PC, Zhang L, et al. Effects of Raf kinase inhibitor protein expression of prostate cancer metastasis. J Natl Cancer Inst 2003;95:878–89.
58. Schuierer MM, Bataille F, Hagan S, Kolch W, Bosserhoff A-K. Reduction in Raf kinase inhibitor protein expression is associated with increased Ras-extracellular signal-regulated kinase signaling in melanoma cell lines. Cancer Res 2004;64:5186–92.